University of Denver

Department of Physics and Astronomy

"Laboratory Studies of Infrared Absorption by NO_2 and HNO_3"

D. G. Murcray, A. Goldman and F. Bonomo

Final Report

NASA Grant 06-004-128

Submitted to

National Aeronautics and Space Administration

Langley Research Center

Hampton, Virginia 23665

I. Introduction

The objective of the research study performed under this grant was to obtain laboratory data concerning the quantitative absorption in the 11 μm and 22 μm region due to HNO_3. These studies were to include obtaining spectra under different temperature conditions so that the temperature dependence of the absorption could be determined. The ultimate objective of the research was to determine the molecular band model parameters and their dependence on temperature in order to accurately predict the emission or absorption due to the HNO_3 in the atmosphere.

As the study was getting under way it was decided that in view of the current interest in stratospheric NO_2 that the study should be expanded to include a laboratory study of the 6.2μ NO_2 band as well as the HNO_3 bands. The first phase of the study consisted of the quantitative studies of the 6.2μ NO_2 band and the 22.0μ HNO_3 bands. The results of this phase have been described in detail in the attached publications. The last phase of the program was devoted to the measurement of the temperature dependence of the 11μ and 22μ HNO_3 bands. The results of these studies are described below.

II. Temperature Dependence of the 11μ and 22μ Bands of HNO_3 Vapor.

The previous laboratory measurements of the 11μ and 22μ HNO_3 bands [2, 3] were made at +40°C. These were extended here to lower temperatures, down to -10°C. The 11μ bands consist of the ν_5 and the $2\nu_9$ transitions while the 22μ bands consist of the ν_9 hot bands. The temperature dependence of the integrated intensity, after the density correction, is 1 for a fundamental band and is larger than 1 for an overtone or a combination band[4, 5]. Over a small range of temperature the deviation from 1 can be neglected. In particular, the temperature dependence for the $2\nu_9$ transition is $[1-\exp(-1.439 \times 458/T(^{\circ}K)]^{-2}\,[1-\exp(-1.439 \times 2 \times 458/T(^{\circ}K)]$,

which varies by only a few percent in the 313-263°K range. In addition, the average spectral line spacing is not expected to vary over a small temperature interval. Therefore the present (S^o/d) measurements at the lower temperatures are expected to increase as 1/T.

Fig 1 shows a quantitative spectrum of the 11μ bands at -10°C under ~0.5cm^{-1} resolution. Comparison with similar spectrum at +40°C (Fig 4, Ref 3) shows no significant changes in the spectral features. Figs 2 and 3 show low resolution quantitative spectra at +10°C and -10°C taken for the purpose of band model analysis. They can be compared with similar spectra at +40°C (Fig 5, Ref 3). The resulting (S^o/d) values are tabulated in Table I and also plotted in Fig 4, together with the values obtained previously at +40°C. It is apparent that the 1/T dependence is verified within the experimental error (5-10%).

Similar data were obtained for the 22μm bands. Fig. 5 shows a quantitative spectrum of the 22μ bands at -10°C under ~0.5cm^{-1} resolution. Fig. 6 shows a number of low resolution spectra of these bands at +10°C. Such spectra were the basis for the band model analysis of the data.

The analysis of the 22μ bands low resolution measurements indicated that for some unclear reason pressure fluctuations occurred during the measurements, especially during the -10°C measurements. As a result, significant fluctations were introduced into the derived ($-\ln\tau/P$) values (where $-\tau$ is the transmittance and P the pressure), and, subsequently, into the curve of growth. Due to these pressure variations the fitting of the experimental data to the theoretical curves of growth was not satisfactory. At a number of frequencies at -10°C no fitting was possible. The resulting S^o/d values, together with these obtained previously at +40°C, are shown in Fig. 7. A relatively large error (approximately a factor of 2), is to be associated with those frequencies for which a fitting was accomplished for both +10°C and -10°C. Due to the large errors involved, no obvious temperature dependence can be concluded at the moment for the 22μ bands.

References

1. A. Goldman, F. S. Bonomo, W. J. Williams and D. G. Murcray, J. Quant. Spectrosc. Radiat. Transfer 15 107 (1975.
2. A. Goldman, F. S. Bonomo, W. J. Williams and D. G. Murcray, J. Opt. Soc. Am. 65, 10 (1975).
3. A. Goldman, T. G. Kyle, and F. S. Bonomo, Appl Opt. 10, 65 (1970).
4. B. L. Crawford, Jr. and H. L. Dinsmore, J. Chem. Phys. 18, 983, 1682 (1950)
5. J. C. Breeze, C. C. Ferriso, C. B. Ludwig and M. Malkmus, J. Chem. Phys. 42, 402 (1965).

Table I. S^{o}/d Values at Several Temperatures for the 11μ HNO_3 Bands.

ν (cm^{-1})	S^{o}/d ($atm^{-1}cm^{-1}$) at +40°C	S^{o}/d ($atm^{-1}cm^{-1}$) at +10°C	S^{o}/d ($atm^{-1}cm^{-1}$) at -10°C
850.0	2.20	2.31	2.29
852.5	2.98	3.17	3.08
855.0	3.91	4.12	4.03
857.5	5.03	5.34	5.25
860.0	6.15	6.59	6.80
862.5	7.27	7.75	8.23
865.0	8.15	8.65	9.30
867.5	8.82	9.24	10.06
870.0	9.22	9.68	10.46
872.5	9.39	9.88	10.57
875.0	9.46	10.05	10.67
877.5	10.55	11.44	12.10
880.0	11.56	13.03	14.06
882.5	11.28	11.80	12.84
885.0	11.10	12.23	13.20
887.5	11.24	12.31	13.50
890.0	11.17	12.30	13.52
892.5	11.57	12.80	14.02
895.0	12.40	13.96	14.89
897.5	12.24	14.53	15.15
900.0	10.49	11.77	12.11
902.5	8.64	9.44	9.91
905.0	7.51	8.05	8.41
907.5	6.84	7.42	8.15

Table I. S^{o}/d Values at Several Temperatures for the 11μ HNO_3 Bands.

ν (cm^{-1})	S^{o}/d ($atm^{-1}cm^{-1}$) at +40°C	S^{o}/d ($atm^{-1}cm^{-1}$) at +10°C	S^{o}/d ($atm^{-1}cm^{-1}$) at -10°C
910.0	6.14	7.02	7.60
912.5	5.66	6.54	6.97
915.0	4.90	5.66	5.89
917.5	3.89	4.31	4.58
920.0	2.87	3.10	3.22

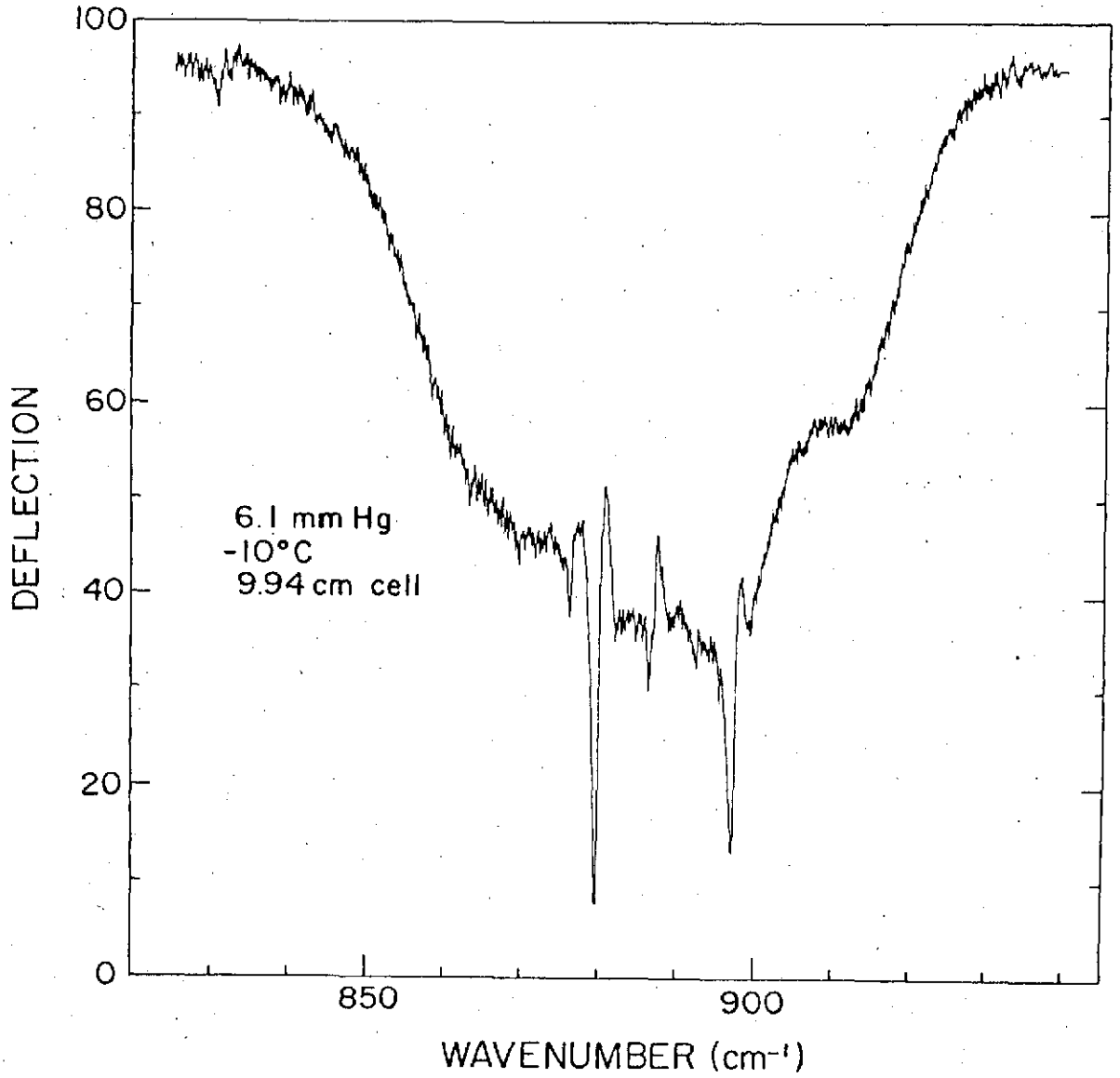
100
80
60
40
20
0
DEFLECTION
6.1 mm Hg
-10°C
9.94 cm cell
850
900
WAVENUMBER (cm⁻¹)

Figure 1.

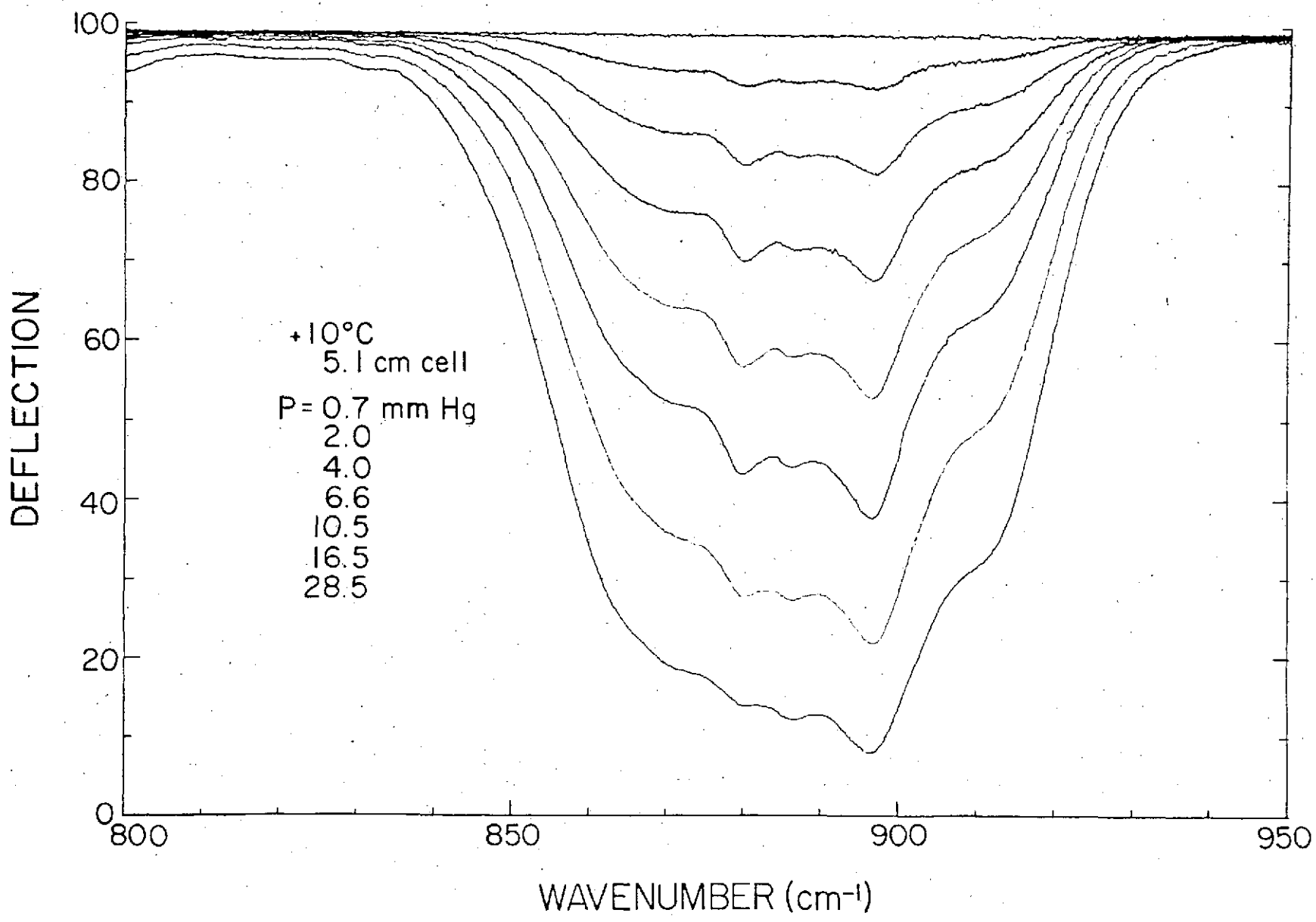
100
80
60
40
20
0
DEFLECTION
+10°C
5.1 cm cell
P = 0.7 mm Hg
2.0
4.0
6.6
10.5
16.5
28.5
800
850
900
950
WAVENUMBER (cm⁻¹)

Figure 2.

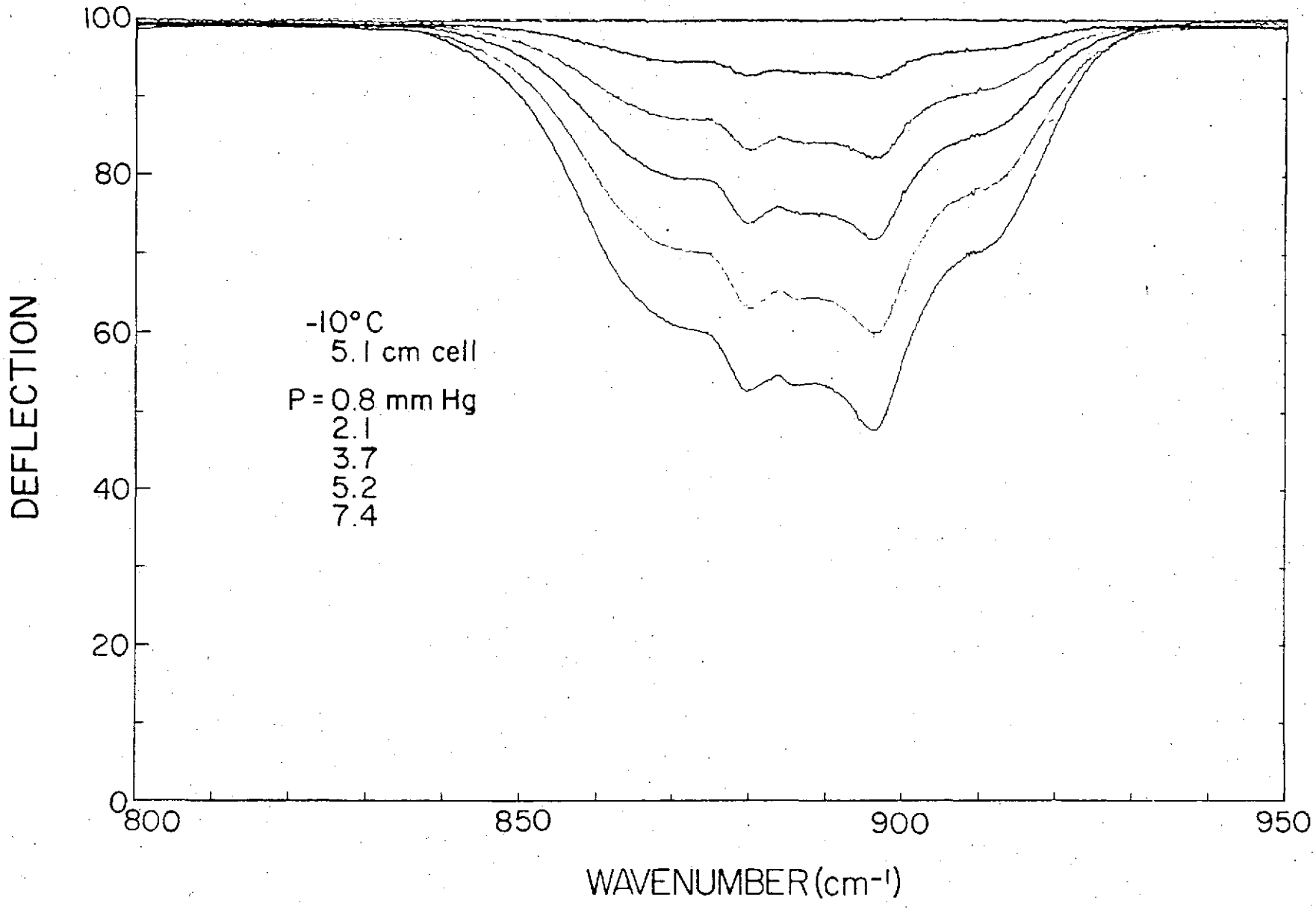
100
80
60
40
20
0
DEFLECTION
-10°C
5.1 cm cell
P = 0.8 mm Hg
2.1
3.7
5.2
7.4
800
850
900
950
WAVENUMBER (cm⁻¹)

Figure 3.

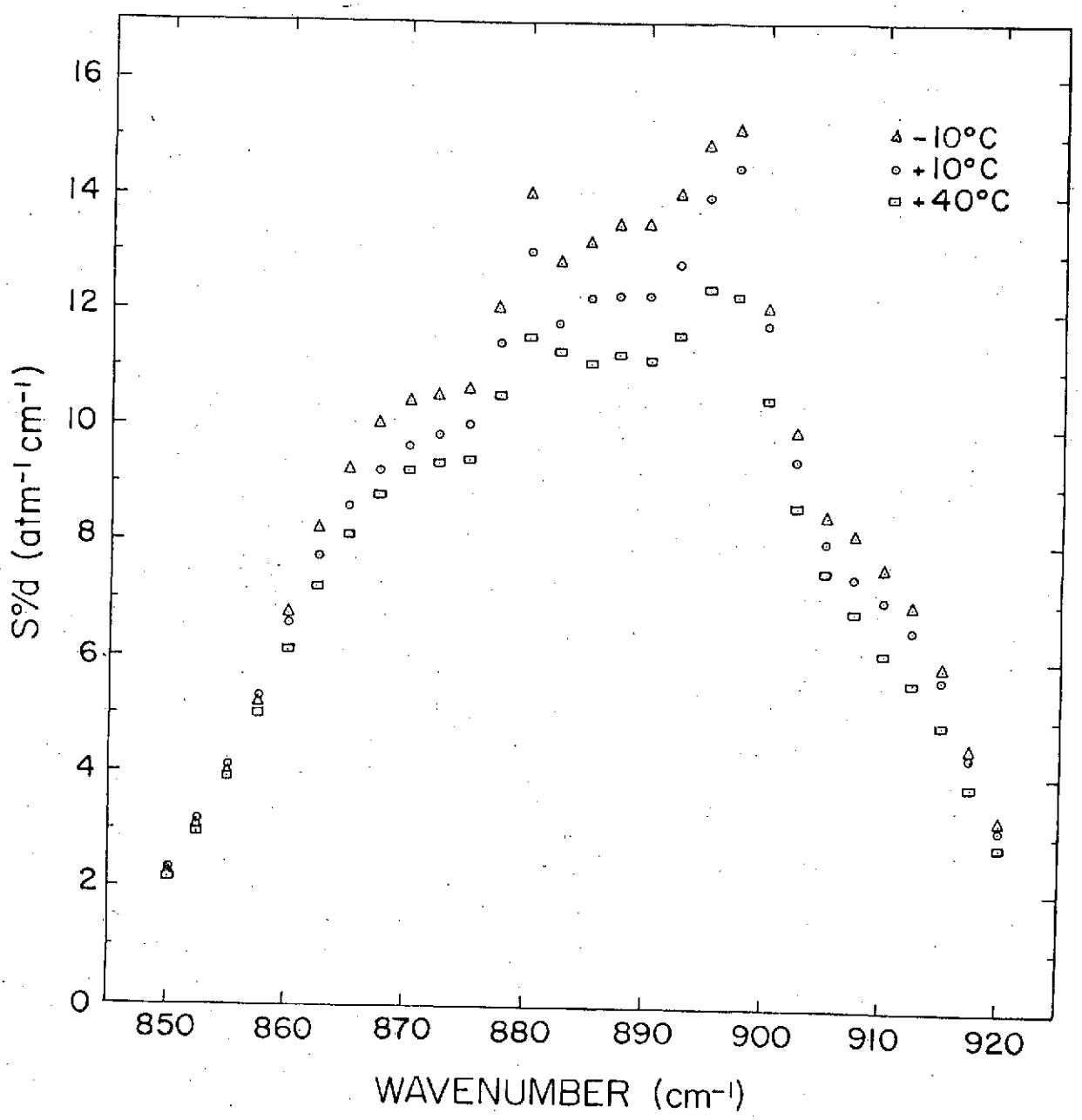
16
14
12
10
8
6
4
2
0
S%d (atm⁻¹ cm⁻¹)
850
860
870
880
890
900
910
920
WAVENUMBER (cm⁻¹)
-10°C
+10°C
+40°C

Figure 4.

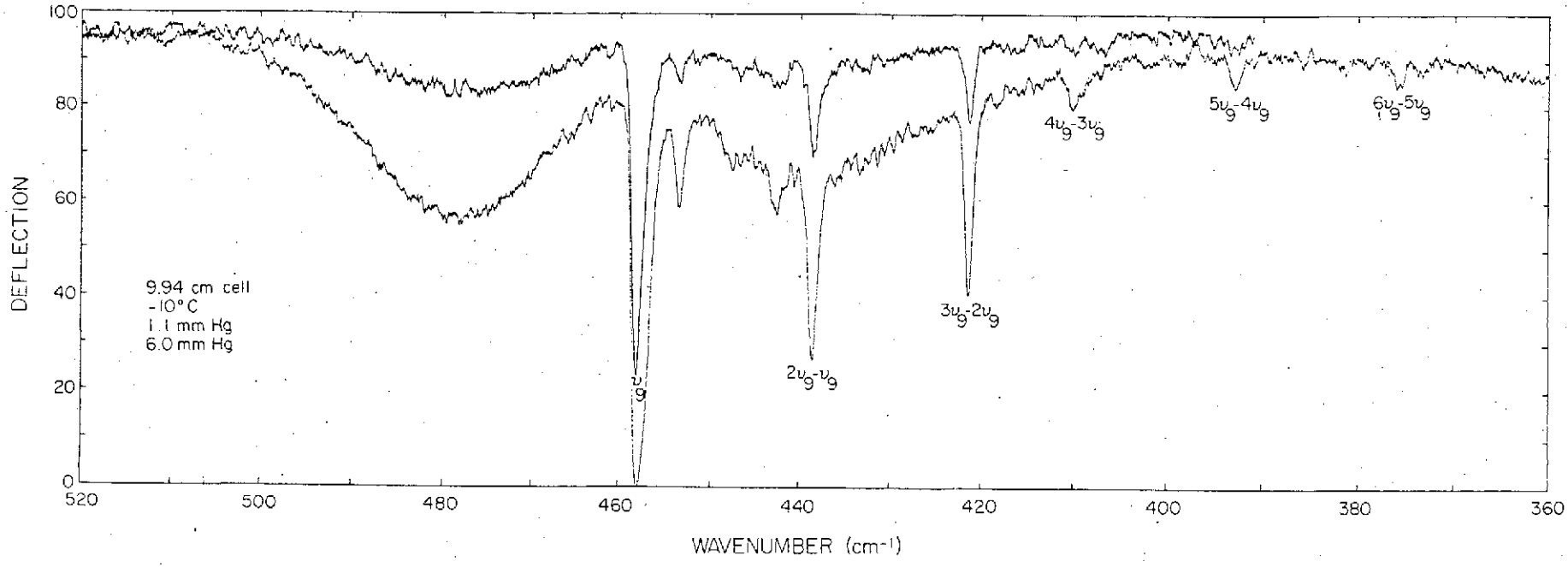
DEFLECTION
WAVENUMBER (cm⁻¹)
9.94 cm cell
-10°C
1.1 mm Hg
6.0 mm Hg
υ_9
$2\upsilon_9$-υ_9
$3\upsilon_9$-$2\upsilon_9$
$4\upsilon_9$-$3\upsilon_9$
$5\upsilon_9$-$4\upsilon_9$
$6\upsilon_9$-$5\upsilon_9$

Figure 5

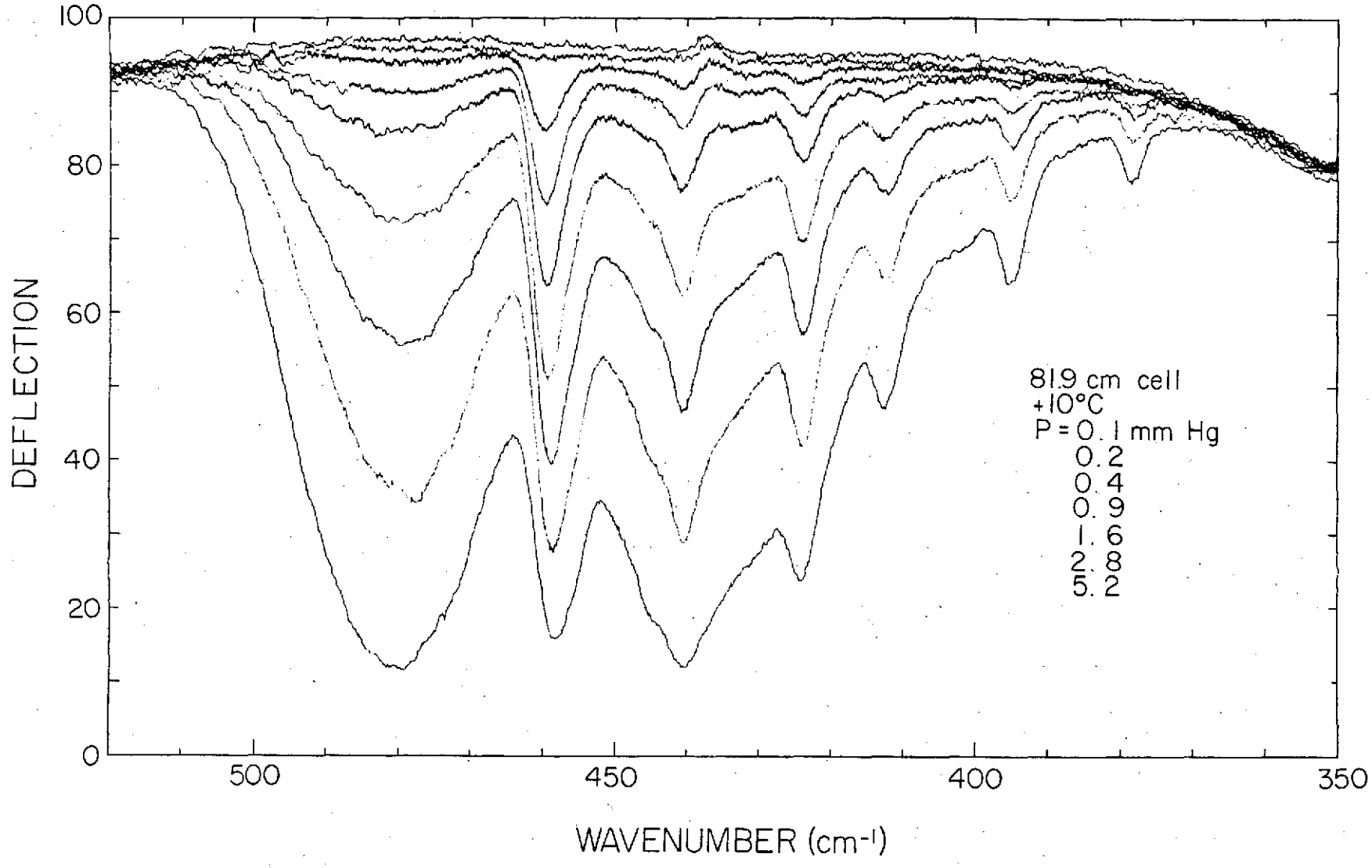
100
80
60
40
20
0
DEFLECTION
500
450
400
350
WAVENUMBER (cm⁻¹)
81.9 cm cell
+10°C
P = 0.1 mm Hg
0.2
0.4
0.9
1.6
2.8
5.2

Figure 6

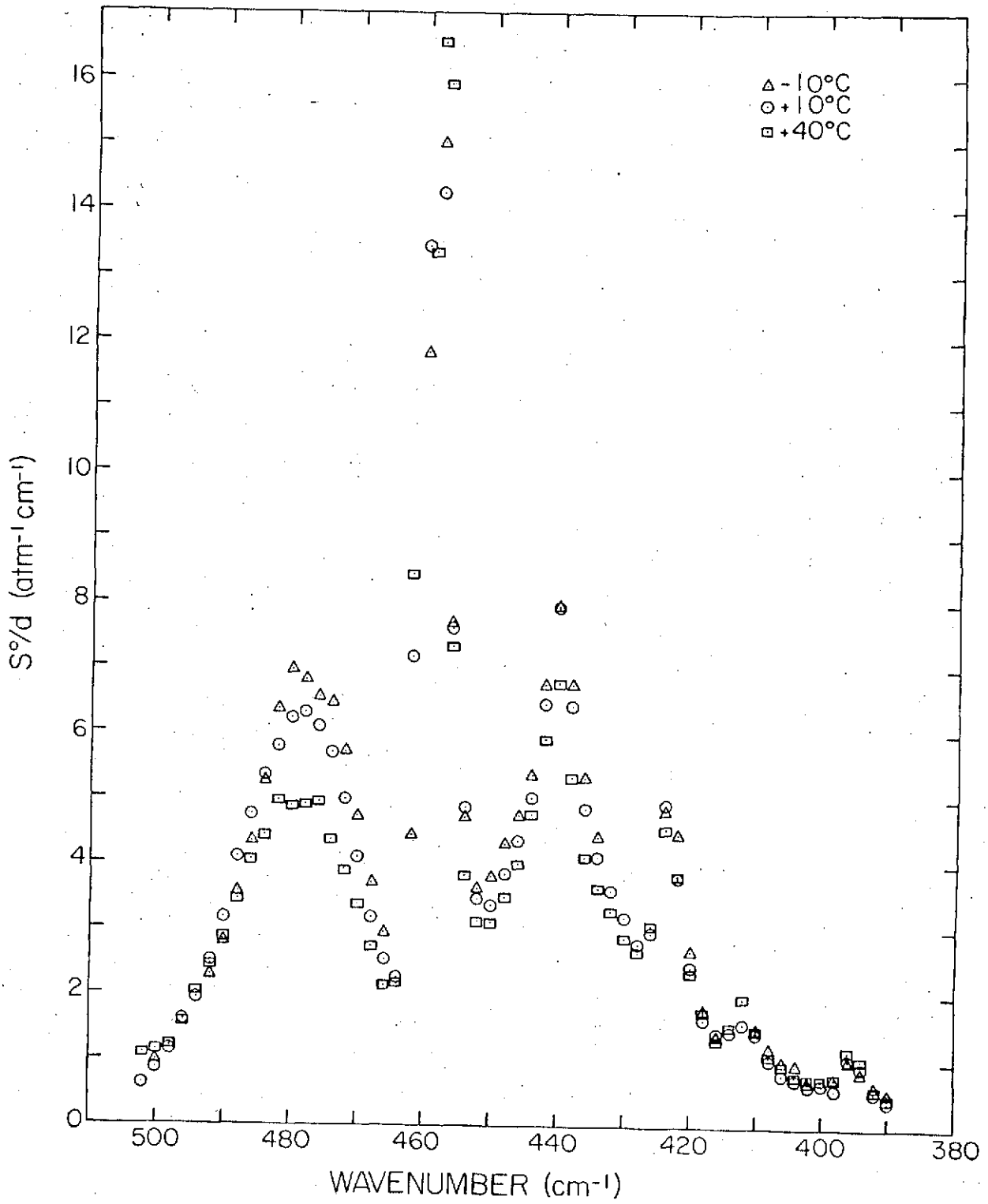
△ -10°C
○ +10°C
□ +40°C
S°/d (atm⁻¹cm⁻¹)
0
2
4
6
8
10
12
14
16
500
480
460
440
420
400
380
WAVENUMBER (cm⁻¹)

Figure 7

Reprinted from:

JOURNAL OF THE OPTICAL SOCIETY OF AMERICA VOLUME 65, NUMBER 1 JANUARY 1975

Statistical-band-model analysis and integrated intensity for the 21.8 μm bands of HNO_3 vapor*

A. Goldman, F. S. Bonomo,† W. J. Williams, and D. G. Murcray

Department of Physics and Astronomy, University of Denver, Denver, Colorado 80210

(Received 2 August 1974)

The 21.8 μm absorption bands of HNO_3 vapor were measured at 40 °C. Statistical-band-model analysis of the data resulted in spectral-band-model parameters and yielded an integrated intensity of 393 ± 15% (cm^{-2} atm^{-1}) at 40 °C between 390 and 502 cm^{-1}.

Index Headings: Absorption; Spectra; Infrared.

Stratospheric HNO_3 was originally detected by the identification of the 7.5 μm vibration–rotation band in the solar spectrum.[1] Subsequently, the 5.9, 11.3, and 21.8 μm HNO_3 bands were also observed in the solar spectrum,[2–7] and the 11.3 and the 21.8 μm bands were observed in atmospheric emission spectra.[4–6] The 11.3 μm band, which is centered at an atmospheric window, has been used extensively for derivation of vertical distributions of HNO_3 in the stratosphere.[4–7]

Atmospheric absorption and emission spectra of the 21.8 μm HNO_3 bands are shown in Figs. 3 and 5 in Ref. 5. Quantitative analysis of such spectra requires laboratory measurements of the spectral absorptivity parameters of these bands. Such parameters were measured and are presented here.

The instrumentation and the experimental and theoretical techniques used in the present study are quite similar to those described previously.[8–11] The spectra were recorded on a double-beam Beckman infrared spectrophotometer Model IR-7, employing a CsI foreprism and grating optics. (In order to obtain high resolution over the CsI region, two orders of grating are utilized; the change occurred at 504 cm^{-1}.) The AgCl cell windows used previously[8] show little transmittance of infrared energy below 450 cm^{-1}, so they were replaced by AgBr windows. Figure 1 shows the HNO_3 vapor survey spectra as measured in the 340–690 cm^{-1} region. Similar spectra for the 600–4000 cm^{-1} region are shown in Ref. 8. Figure 1 shows that the 21.8 μm bands extend from about 360 to about 520 cm^{-1}. H_2O vapor lines that were superimposed on the same chart allow an improved wavenumber calibration and show the overlapping regions between HNO_3 and H_2O lines. This occurs mostly at the HNO_3 ν_9, $3\nu_9$-$2\nu_9$, and $6\nu_9$-$5\nu_9$ Q-branch peaks. H_2O calibration spectra under similar resolution and gas amount are given in Ref. 12. The spectral resolution of ~1 cm^{-1} does not allow a clear separation of the groups of the HNO_3 rotational lines, spaced at approximately 0.8 cm^{-1}, which were observed in the balloon-flight data.[5] This spacing is in agreement with a C-type rigid-rotor approximation for the HNO_3 ν_9 fundamental band, as the rotational constants are[13] $A \approx B \approx 0.4$ cm^{-1}. The optical path used in Fig. 1 allows for the identification of a number of hot bands on the low-wave-number side of the ν_9 fundamental band. The measured Q-branch peaks (within ±0.1 cm^{-1}) occur at 457.8, 438.5, 422.1, 410.5, 392.8, and 376.5 cm^{-1} for the ν_9, $2\nu_9$-ν_9, $3\nu_9$-$2\nu_9$, $4\nu_9$-$3\nu_9$, $5\nu_9$-$4\nu_9$, and $6\nu_9$-$5\nu_9$ bands, respectively. These values include more hot bands than those observed earlier,[14] and should be useful for a more-detailed vibrational analysis. The first two of the hot bands, i.e., $2\nu_9$-ν_9 and $3\nu_9$-$2\nu_9$, are also observed on the atmospheric absorption shown in Fig. 3 of Ref. 5. The first hot band is also clearly observed in atmospheric emission; the second one, which is close to a strong H_2O line group, is smoothed out by the spectrometer slit function (Fig. 5 of Ref. 5).

A large number of low-resolution (~7 cm^{-1}) quantitative spectra were obtained for a band-model analysis of the 21.8μm bands by using five different absorption cells and numerous gas pressures. The 0.5, 1.0, and 2.0 cm cells were made from Teflon, and the 5.10 and 9.94

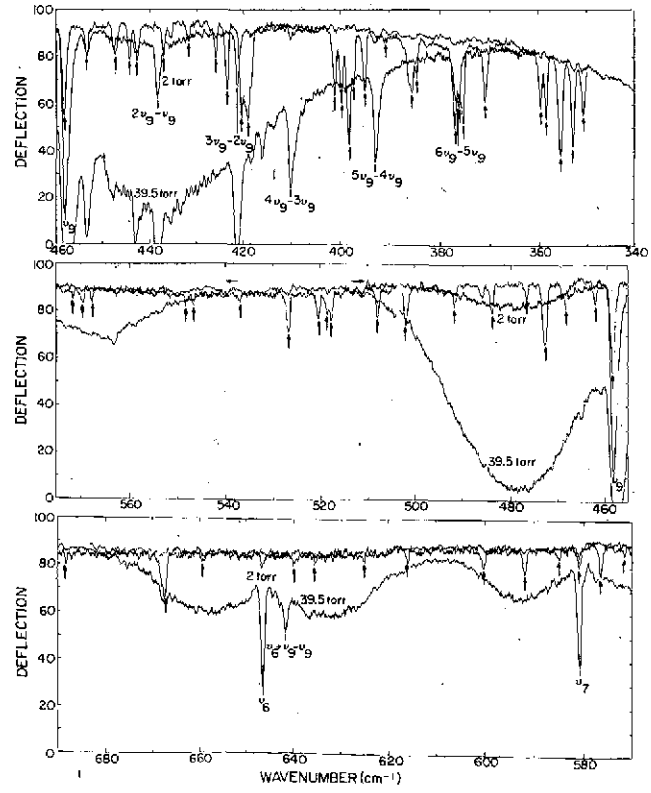

FIG. 1. Spectra of HNO_3 vapor in the 340–690 cm^{-1} region at ~1 cm^{-1} resolution obtained with the 9.94 cm cell. The upper HNO_3 spectrum is at 2.0 torr; the lower is at 39.5 torr, and both are at 40 °C. The low-pressure spectrum was deleted from 510 to 540 cm^{-1} (horizontal arrows) because it does not have a measured absorption. H_2O lines, denoted by vertical arrows, are superimposed on the HNO_3 spectra.

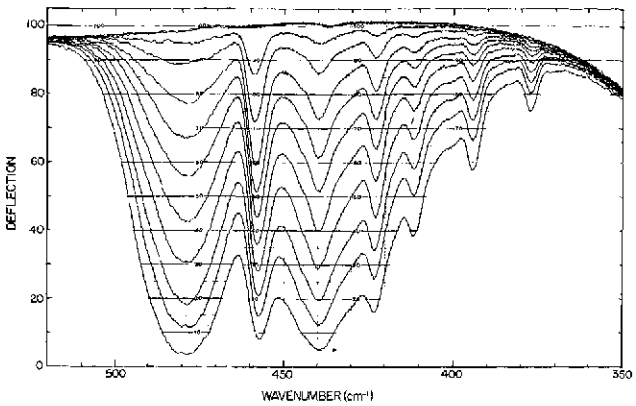

FIG. 2. Low-resolution (~7 cm^{-1}) spectra of HNO_3 vapor at 40 °C in the 9.94 cm cell. Pressures from the top are 1.2, 2.5, 4.9, 7.5, 10.5, 15.0, 21.0, 34.5, 38.0, and 51.5 torr.

cm cells were made from Pyrex glass. Some of the spectra produced are shown in Figs. 2 and 3. These were made with pure HNO_3 vapor at 40 °C, with pressures ranging from a few torr to near saturation pressures. The saturation pressure at room temperature[15] dictated the maximum absorption that could be obtained with a given cell.

The spectral curve of growth analysis was applied to ~70 frequencies within the band, at ~2 cm^{-1} intervals to closely follow the shape of the absorption curves. Fitting $-\ln\bar{T}/p$ vs L [where $\bar{T}$ is the observed average transmittance, p (atm) is the pressure, and L (cm) is the cell length] to a two-parameter model (with Lorentz line shape)[6] yielded the band-model parameters, α_ν (cm^{-1}) and β_ν^0 (atm^{-1}). Their product, which yields $(S^0/d)_\nu$ ($cm^{-1}\,atm^{-1}$), is shown in Fig. 4. This analysis showed that for most frequencies within the band, the absorption is in the linear and intermediate regions of the curve of growth. The exception is the ν_9 Q-branch, in which the absorption is in the intermediate and square-root region, with $\alpha_\nu = 0.486$ cm^{-1}, $\beta_\nu^0 = 34.1$ atm^{-1}, and $(S^0/d)_\nu = 16.5$ $cm^{-1}atm^{-1}$. As a result, the accuracy of $(S^0/d)_\nu$ is significantly larger than that of α_ν and β_ν^0.[8] Fitting $-\ln\bar{T}/p$ vs L to a three-parameter model (with Voigt line shape)[9,11] yielded the same values for α_ν and β_ν^0 and, in addition, values for δ_ν^0. In principle, this allows the estimation of the Lorentz half-width. However, the corresponding δ_ν values are $\gg 1$ so that the fitting is not sensitive to this parameter.

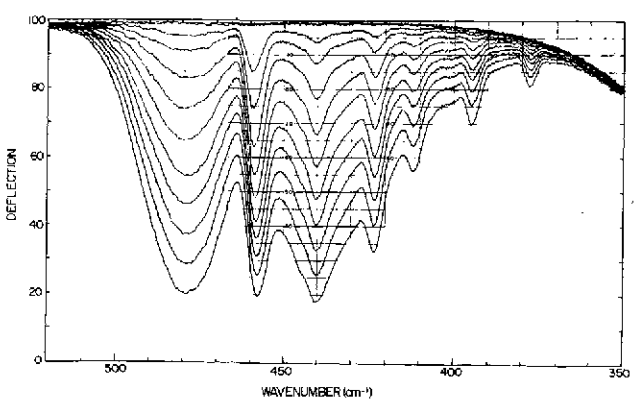

FIG. 3. Low-resolution (~7 cm^{-1}) spectra of HNO_3 vapor at 40 °C in the 5.10 cm cell. Pressures from the top are 1.4, 3.3, 6.7, 12.0, 16.5, 24.0, 29.0, 36.0, 45.5, and 55.5 torr.

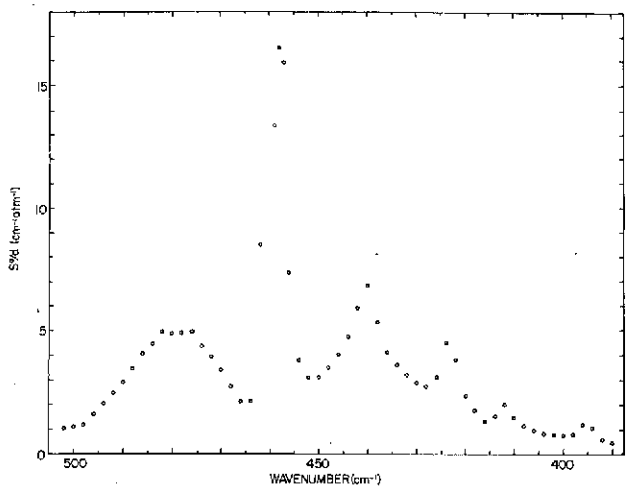

FIG. 4. $(S^0/d)_\nu$ for the 21.8 μm HNO_3 bands in the 390–502 cm^{-1} region.

The integrated intensity S_b^0 ($cm^{-2}\,atm^{-1}$, at 40 °C) of the 21.8 μm bands was derived in two ways[8]: one from $S_b^0 = \int_{\nu 1}^{\nu 2} (S^0/d)_\nu d\nu$, and one from $S_b^0 = (-1/pL)\int_{\nu 1}^{\nu 2} \ln\bar{T}(\nu)\,d\nu$ of the short cell. These gave 393 ± 15% and 404 ± 20% ($cm^{-2}\,atm^{-1}$), respectively, between $\nu_1 = 390$ cm^{-1} and $\nu_2 = 502$ cm^{-1}. As discussed previously,[8] the first of the two values should be regarded as the best value for the integrated intensity.

Although the temperature of the gas samples used in the present study is higher than the lower stratospheric temperature, it is expected that the present results will be useful in the analysis of absorption and emission spectra of the lower stratosphere in the 20–24 μm region. In particular, these results, in addition to those from the 11.3 μm band,[4-7] can be used for an independent determination of HNO_3 vertical distribution. Careful attention should be given, however, to the interference between the HNO_3 and the H_2O lines in this spectral region.

ACKNOWLEDGMENTS

Acknowledgment is made to the National Center for Atmospheric Research, which is sponsored by the National Science Foundation, for computer time used in this research. The figures were carefully prepared by Carolyn Bauer.

*Supported in part by NASA Langley Research Center.

†Chemistry Div., Denver Research Institute, University of Denver.

[1]D. G. Murcray, T. G. Kyle, F. H. Murcray, and W. J. Williams, Nature 218, 78 (1968).

[2]D. G. Murcray, T. G. Kyle, F. H. Murcray, and W. J. Williams, J. Opt. Soc. Am. 59, 1131 (1969).

[3]D. G. Murcray, F. H. Murcray, W. J. Williams, T. G. Kyle, and A. Goldman, Appl. Opt. 8, 2519 (1969).

[4]W. J. Williams, J. N. Brooks, D. G. Murcray, F. H. Murcray, P. M. Fried, and J. A. Weinman, J. Atmos. Sci. 29, 1375 (1972).

[5]J. N. Brooks, A. Goldman, J. J. Kosters, D. G. Murcray, F. H. Murcray, and W. J. Williams, in *Physics and Chemis-*

try of Upper Atmospheres, edited by B. M. McCormac (Reidel, Dordrecht, Holland, 1973), p. 278.
[6]D. G. Murcray, A. Goldman, A. Csoeke-Poeckh, F. H. Murcray, W. J. Williams, and R. N. Stocker, J. Geophys. Res. 78, 7033 (1973).
[7]D. G. Murcray, A. Goldman, W. J. Williams, F. H. Murcray, J. N. Brooks, J. Van Allen, R. N. Stocker, J. J. Kosters, D. B. Barker, and D. E. Snider, in *Proceedings of the Third Conference on the Climatic Impact Assessment Program*, edited by A. J. Broderick (U.S. Dept. of Transportation, Cambridge, Mass., 1974).
[8]A. Goldman, T. G. Kyle, and F. S. Bonomo, Appl. Opt. 10, 65 (1971).
[9]A. Goldman and S. C. Schmidt, J. Quant. Spectrosc. Radiat. Transfer 13, 709 (1973).
[10]A. Goldman, F. S. Bonomo, W. J. Williams, D. G. Murcray, and D. E. Snider, J. Quant. Spectrosc. Radiat. Transfer (1974).
[11]S. C. Schmidt, A. Goldman, F. S. Bonomo, D. G. Murcray, and R. C. Amme, Appl. Opt. 13, 1202 (1974).
[12]L. R. Blaine, E. K. Plyler, and W. S. Benedict, J. Res. Natl. Bur. Std. 66A, 223 (1962).
[13]A. P. Cox and J. M. Riveros, J. Chem. Phys. 42, 3106 (1965).
[14]G. E. McGraw, D. L. Bernitt, and I. C. Hisatsune, J. Chem. Phys. 42, 237 (1965).
[15]S. A. Stern, J. T. Mullhaupt, and W. B. Kay, Chem. Rev. 60, 185 (1960).

Reprinted from

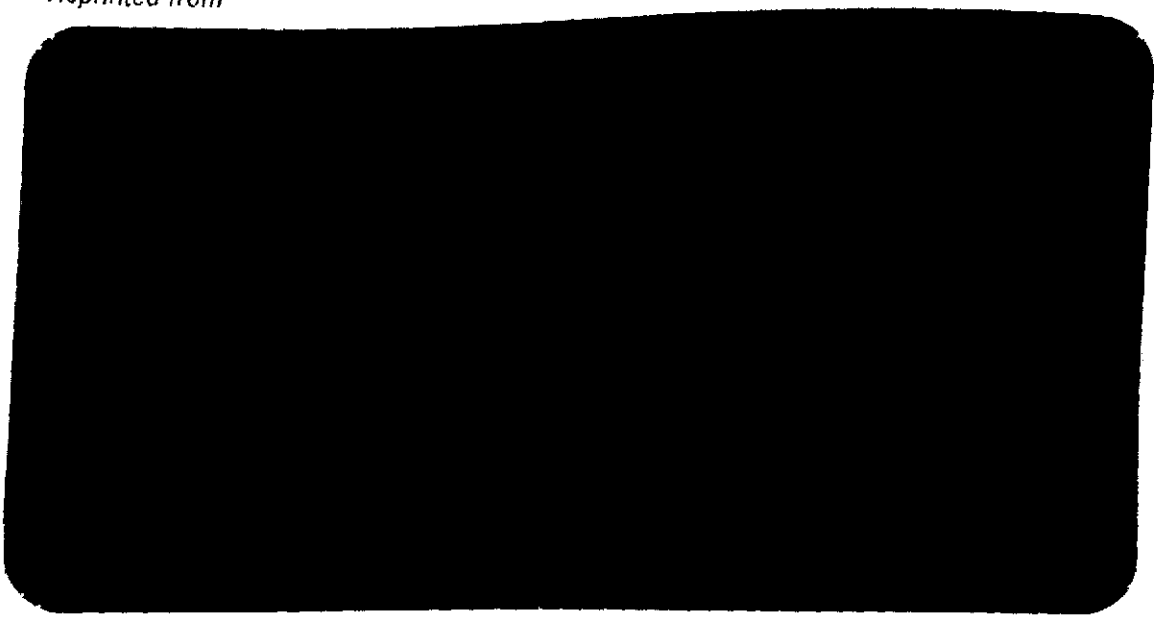

PERGAMON PRESS
OXFORD · NEW YORK

J. Quant. Spectrosc. Radiat. Transfer. Vol. 15, pp. 107–112. Pergamon Press 1975. Printed in Great Britain.

ABSOLUTE INTEGRATED INTENSITY AND INDIVIDUAL LINE PARAMETERS FOR THE 6·2μ BAND OF NO_2*

A. GOLDMAN, F. S. BONOMO†, W. J. WILLIAMS and D. G. MURCRAY
Department of Physics and Astronomy, University of Denver, Denver, Colorado 80210, U.S.A.
and
D. E. SNIDER
Ballistic Research Laboratories, Aberdeen Proving Ground, Maryland 21005, U.S.A.

(*Received* 13 *May* 1974)

Abstract—The absolute integrated intensity of the 6·2μ band of NO_2 at 40°C was determined from quantitative spectra at ~10 cm^{-1} resolution by the spectral band model technique. A value of 1430 ± 300 cm^{-2} atm^{-1} was obtained. Individual line parameters, positions, intensities and ground state energies were derived, and line-by-line calculations were compared with the band model results and with the quantitative spectra obtained at ~0·5 cm^{-1} resolution.

1. INTRODUCTION

SINCE the identification of the ν_3 NO_2 band in the solar spectrum, as observed from a balloon-borne spectrometer,[1] this band has become of considerable importance for spectroscopic studies of NO_2 in the atmosphere.[2] The quantitative analysis of atmospheric ν_3 NO_2 data requires a precise knowledge of the spectral-line parameters, i.e. line positions, absolute intensities, halfwidths and ground state energies. A successful rotational analysis of this band was accomplished only recently by HURLOCK *et al.*,[3] from which the line positions, ground state energies and relative intensities can be computed. However, there exists only the measurement of the total band intensity[4] to which the individual relative intensities must be normalized.

In the present work, we have remeasured the 6·2μ NO_2 band intensity from quantitative spectra obtained with several absorption cells. These spectra permitted the total band intensity as well as an estimate of the self broadened Lorentz halfwidth to be determined, using spectral band model analysis of ~10 cm^{-1} resolution spectra. These results and the recently derived rotational constants[3] were used to generate individual line parameters for the ν_3 $^{14}N^{16}O_2$ band. The derived line parameters were used for spectral comparisons with the band model results and with quantitative spectra obtained at ~0·5 cm^{-1} resolution.

2. MEASUREMENTS AND BAND MODEL ANALYSIS

The experimental procedure, instrumentation and methods of analysis used in the present study have been described in detail in previous publications.[5–7] The spectral band model analysis of laboratory data has been described for spectral lines with either Lorentz or Voigt shape.[5,6]

*Supported in part by NASA Langley Research Center and in part by Ballistic Research Laboratories, Aberdeen Proving Ground.

†Chemistry Division, Denver Research Institute, University of Denver.

The spectra were recorded on a double-beam Beckman infrared spectrophotometer, Model IR-7, at 40°C. A total of four cells was used, all with AgCl windows. The 0·5 cm and 2·0 cm cells were made from Teflon, and the 4·96 cm and 9·94 cm cells were made from Pyrex glass. The NO_2 samples used were CP grade from the Matheson Company. No foreign gases were introduced into the absorption cells. Numerous spectra were recorded at $\sim 10\,cm^{-1}$ resolution and at $\sim 0{\cdot}5\,cm^{-1}$ resolution with various pressures from ~3 to ~300 mm Hg. The pressures were read using both a standard mercury-filled manometer with a small layer of Kel-F fluorocarbon oil protecting the mercury, and a differential manometer filled with the same oil.

Quantitative NO_2 analysis of these absorption spectra is complicated by the fact that NO_2 dimerizes according to $2NO_2 \rightleftarrows N_2O_4$. In addition, a small impurity of HNO_3 was also present in the spectra. The HNO_3 and N_2O_4 contaminations were monitored by scanning the 1670–1800 cm^{-1} region at $\sim 0{\cdot}5\,cm^{-1}$ resolution, which showed both the 1750 cm^{-1} N_2O_4 band and the 1712 cm^{-1} HNO_3 band. HNO_3 and N_2O_4 bands, however, do not overlap the ν_3 band of $^{14}N^{16}O_2$.

The band model curve-of-growth analysis was applied to the $\sim 10\,cm^{-1}$ resolution spectra. A typical set of spectra as obtained in one of the four cells is shown in Fig. 1. In order to minimize the effects of the dimerization, the analysis was applied to data obtained with pressures less than 100 mm Hg. At a total pressure of 100 mm Hg and at 40°C, the ratio of NO_2 to N_2O_4 is 4:1, as calculated from the known equilibrium constant.[8] As the pressure decreases, the NO_2 proportion increases significantly (larger proportions of NO_2 with little N_2O_4 dimerization can be obtained at higher temperatures). The NO_2 pressures were also corrected for the HNO_3 contamination which was estimated as less than 5 per cent of the total pressure.

The curve-of-growth analysis was applied to ~40 frequencies within the band, at $\sim 3\,cm^{-1}$ intervals, so that the selected net of frequencies closely followed the shape of the transmittance curves. For each selected frequency $\nu(cm^{-1})$, the observed $-\ln \bar{T}(\nu)/P$ (where $\bar{T}$ is the average transmittance and P is the NO_2 pressure) was fitted to a curve-of-growth with a Voigt profile, as described in detail in the previous publications.[6,7] This analysis yields values for the band model parameters $\alpha(\nu)(cm^{-1})$, $\beta°(\nu)(atm^{-1})$ and $d°(\nu)(atm^{-1})$,[5–7] shown in Fig. 2. A typical fitting of $-\ln \bar{T}(\nu)/P$ for one point of Fig. 2 (at $\nu = 1630\,cm^{-1}$) is shown in Fig. 3. The variance of this fitting is ~4 per cent.

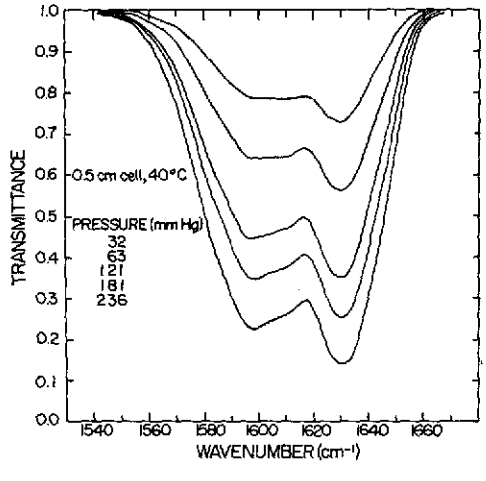

Fig. 1. Typical set of ~10 cm^{-1} resolution spectra of the 6·2μ NO_2 band.

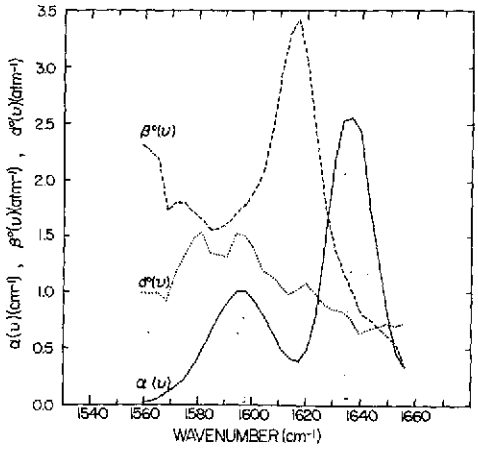

Fig. 2. Spectral band model parameteters $\alpha(\nu)$, $\beta^\circ(\nu)$ and $d^\circ(\nu)$ derived for the 6·2μ NO_2 band. The vertical scale applies to $\alpha(\nu)$ and is to be multiplied by 10 and 100 for $\beta^\circ(\nu)$ and $d^\circ(\nu)$ respectively.

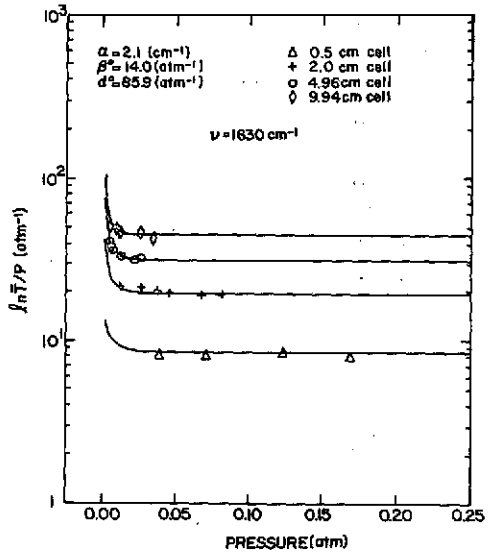

Fig. 3. $-\ln \bar{T}(\nu)/P$ vs P for $\nu = 1630\,\text{cm}^{-1}$.

In Fig. 2, $\beta^\circ(\nu)$ is proportional to the ratio of the average Lorentz halfwidth and the average line spacing. The peak in the $\beta^\circ(\nu)$ curve near 1615 cm^{-1} indicates high density of the spectral lines. This could be due to the Q-branches in this region (see Fig. 4), as well as possible spin splitting effects and "hot" bands contribution. The quantity $\alpha(\nu)L$, where L is the cell length, yields the Ladenburg–Reiche parameter; therefore[5] the $\alpha(\nu)$ curve indicates that the present experimental data fall mostly in the intermediate region of the curve-of-growth. The parameter $d^\circ(\nu)$ is proportional to the ratio of the average Lorentz halfwidth to the Doppler halfwidth; thus it can be used to derive the variation of the average Lorentz halfwidth across the band. However, Fig. 3 indicates that the fitted curvature in the Doppler region is not supported by sufficient data

points. In this regard it should be noted here that fitted $d^\circ(\nu)$ values greater than ~100 are uncertain. This is due to the fact that, even for the lower pressures pressures (~5 mm Hg) used for the present spectra, the Lorentz halfwidth is still of the order of the Doppler halfwidth so that the Lorentz shape contribution dominates the Voigt shape. As a result, the fitted curves-of-growth are not very sensitive to $d^\circ(\nu) \geq 100$ and the corresponding Lorentz halfwidths [derived from $d^\circ(\nu)$] are uncertain. It is estimated that the average self-broadened Lorentz halfwidth is 0·08 cm^{-1} atm^{-1} ±50 per cent at 40°C. This result indicates the possibility of a higher value than the theoretical estimate of 0·06 cm^{-1} atm^{-1} at 300°K.[9] Sensitivity tests show that the results for $\alpha(\nu)$ and $\beta^\circ(\nu)$ are practically independent of $d^\circ(\nu)$ when $d^\circ(\nu) \geq 100$. This conclusion has also been verified by fitting the data outside the Doppler region to the spectral band model with a Lorentz line shape, i.e. a two parameter model with the same $\alpha(\nu)$ and $\beta^\circ(\nu)$ as above.[5] Further sensitivity tests of the fitted band model parameters verified that $(S^\circ/d)_\nu = \alpha(\nu)\beta^\circ(\nu)$ is the most accurate parameter derived in the present analysis.[5]

The integrated intensity for the total band is then obtained by the $\int (S^\circ/d)_\nu \, d\nu$ over the band. The area under the $(S^\circ/d)_\nu$ curve yields an estimate of 1430 ± 300 cm^{-2} atm^{-1} for the band intensity at 40°C. This includes an additional 12 per cent estimated from the spectra in the shortest cell for band wings not covered in the band model analysis. This band intensity is lower than that of 2059 cm^{-2} atm^{-1} at 25°C derived by GUTTMAN.[4] It is interesting to note that the present curve-of-growth analysis clearly confirms that the small cell length used by GUTTMAN (0·045 cm) is in the linear region of the curve-of-growth so that his derivation of the band intensity from the $-\int \ln \bar{T}(\nu) \, d\nu / P(NO_2)L$ curve should definitely yield the correct band intensity. The source of the disagreement is not clear, but may be due to differences between GUTTMAN'S and the present determinations of the NO_2 gas amounts in the absorption cells. However, GUTTMAN's work yielded the generally accepted heat of dissociation for N_2O_4,[10] and his observed temperature dependence for the band intensity verifies the correct change in gas composition with temperature.

3. SPECTRAL LINE PARAMETERS

Individual line positions, relative intensities, and ground state energies were computed for $^{14}N^{16}O_2$, and were then normalized to the total band intensity of 1430 cm^{-2} atm^{-1}. Upper and lower state rotational energy levels for $J \leq 60$ and $K_{-1} \leq 12$ were computed from the constants of HURLOCK *et al.*[3] Due to the zero spin of the ^{16}O nuclei, only symmetric lower-state rotational energy levels are populated. Type A selection rules (with $\Delta K_{-1} = \pm 1$) were applied to obtain the allowed transitions, for which rigid asymmetric rotor relative line intensities were assumed. Neither "hot" bands [the strongest, $(\nu_3 + \nu_2 - \nu_2)$, contributing about 5 per cent] nor isotopic bands were included in this compilation. Spin splitting, due to an unpaired electron, has been observed in ν_3 of $^{14}N^{16}O_2$, but was not included in the rotational analysis.[3] Nor was it taken into account in the present calculations. Figure 4 shows the derived line intensities as a function of wavenumber ν. A number of K_{-1} sub-bands as well as Q-branches can be seen. Due to the relatively large difference in the rotational constant A in the lower and upper states, the Q-branches do not form a central feature, but are spread out on the low wavenumber side of band center.

The statistical band model parameters $\alpha(\nu)$, $\beta^\circ(\nu)$ and $d^\circ(\nu)$ can be calculated theoretically from the individual line parameters and the half-widths.[11] In particular, $(S^\circ/d)_\nu$ is given by $\Sigma_i S_i^\circ/\Delta\nu$, where the sums are taken over all spectral lines in the spectral interval $\Delta\nu(cm^{-1})$. Figure 5 shows a comparison between the calculated and the experimental values of $(S^\circ/d)_\nu$ for 40°C and $\Delta\nu = 10$ cm^{-1}. Such a comparison is independent of the halfwidths and the spin splitting. It is interesting to note that good agreement is obtained in the R-branch and in the wings, but that the

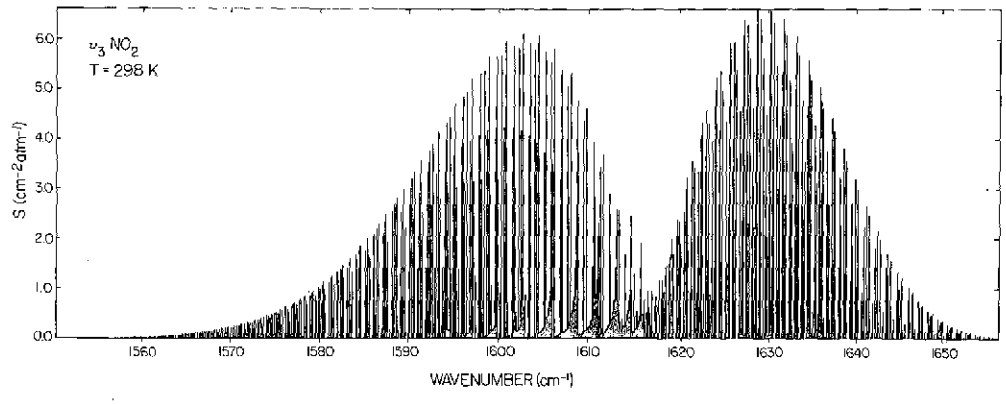

Fig. 4. Line intensities for the ν_3 $^{14}N^{16}O_2$ band at 298°K.

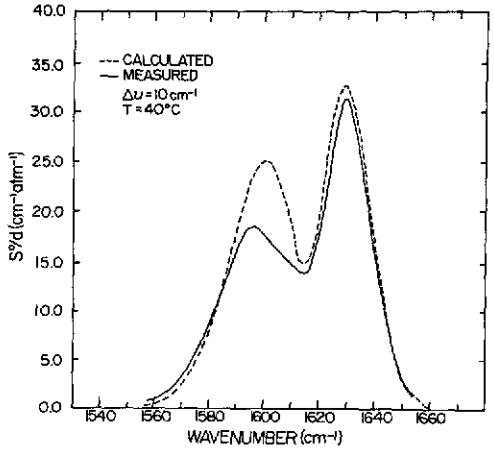

Fig. 5. Comparison of calculated and observed values of $(S°/d)_\nu$.

calculated values are larger than the experimental values in the P-branch. The calculated individual line intensities, which are normalized to 1430 cm^{-2} atm^{-1}, do not yield significant $(S°/d)_\nu$ values outside the wavenumber interval covered by the experimental $(S°/d)_\nu$, even though the experimental spectra indicate larger wings.

The derived line parameters were also used in comparisons of line-by-line calculations with the experimental spectra. A typical comparison is shown in Fig. 6, where 0·5 cm^{-1} and 10 cm^{-1} resolution have been assumed in the calculated spectra respectively. An average halfwidth of 0·1 cm^{-1} atm^{-1} at 300°K has been assumed for all lines. It is seen that most of the observed spectral structure is reproduced by the spectra calculated on the line-by-line basis. However, the observed spectrum shows 5–10 per cent more absorption than the calculated spectrum, which may suggest that the present band intensity is too low. Another possible contribution to this difference can be due to even larger halfwidth and due to spin splitting. Including spin splitting in the line compilation is expected to increase the calculated absorption for splittings larger than the

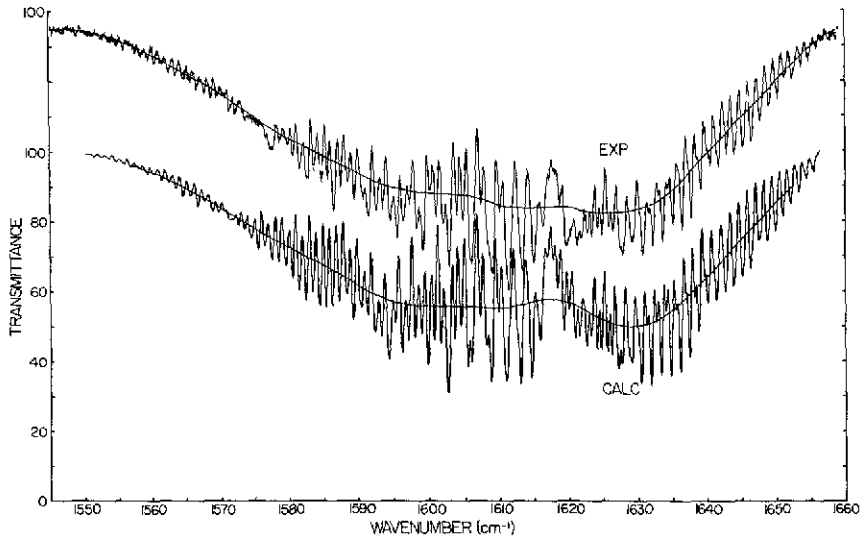

Fig. 6. Comparison of theoretical and experimental spectra at ~0·5 cm^{-1} and ~10 cm^{-1} resolutions for the 6·2μ NO_2 band at 40°C, 21 mm Hg and 4·96 cm cell. The 100 per cent line is displaced by 40 per cent for clarity. (The smoother curve corresponds to the 10 cm^{-1} resolution.)

halfwidths. This effect has been verified by recent 6·2μ NO_2 line-by-line calculations by J. SUSSKIND.[12] Unfortunately, no reliable spin splitting parameters are available at this time.

Acknowledgements—The authors are indebted to S. C. HURLOCK, W. J. LAFFERTY and K. NARAHARI RAO for making their ν_3 NO_2 analysis available prior to publication.

Acknowledgment is made to the National Center for Atmospheric Research, which is sponsored by the National Science Foundation, for computer time used in this research.

Acknowledgment is also made to the Computer Support Division of the Ballistic Research Laboratories, Aberdeen Proving Ground, for assistance with many of the computations.

REFERENNCES

1. A. GOLDMAN, D. G. MURCRAY, F. H. MURCRAY, W. J. WILLIAMS and F. S. BONOMO, *Nature, Lond.* **225**, 443 (1970).
2. D. G. MURCRAY, A. GOLDMAN, W. J. WILLIAMS, F. H. MURCRAY, J. N. BROOKS, J. VAN ALLEN, R. N. STOCKER, J. J. KOSTERS, D. B. BARKER and D. E. SNIDER, Recent Results of Stratospheric Trace Gas Measurements from Balloon-Borne Spectrometers, Proceedings of the Third Conference on the Climatic Impact Assessment Program, in press (1974).
3. S. C. HURLOCK, W. J. LAFFERTY and K. NARAHARI RAO, *J. molec. Spectrosc.* **50**, 246 (1974).
4. A. GUTTMAN, *JQSRT* **2**, 1 (1962).
5. A. GOLDMAN, T. G. KYLE and F. S. BONOMO, *Appl. Opt.* **10**, 65 (1971).
6. A. GOLDMAN and S. C. SCHMIDT, *JQSRT* **13**, 709 (1973).
7. S. C. SCHMIDT, A. GOLDMAN, F. S. BONOMO, D. G. MURCRAY and R. C. AMME, *Appl. Opt.* **13**, 1202 (1974).
8. K. SCHOFIELD, *J. phys. Chem.* Ref. Data **2**, 25 (1973).
9. G. D. T. TEJWANI, *J. chem. Phys.* **57**, 4676 (1972).
10. A. GUTTMAN and S. S. PENNER, *J. chem. Phys.* **36**, 98 (1962).
11. A. GOLDMAN and T. G. KYLE, *Appl. Opt.* **7**, 1167 (1968).
12. J. SUSSKIND, private communication (1974).